Syntheses, Structures, and Stabilities of $[PPh_4][WS_3(SR)]$ (R = ^{i}Bu, ^{i}Pr, ^{t}Bu, Benzyl, Allyl) and $[PPh_4][MoS_3(S^tBu)]$

Naomi L. Kruhlak, Meiping Wang, P. Michael Boorman,* and Masood Parvez

Department of Chemistry, University of Calgary, Calgary, Alberta, Canada, T2N 1N4

Robert McDonald

Department of Chemistry, University of Alberta, Edmonton, Alberta, Canada, T6G 2G2

Received August 22, 2000

Intermediates in the condensation process of $[MS_4]^{2-}$ (M = Mo, W) to polythiometalates, in the presence of alkyl halides, had not been reported prior to our communication of $[PPh_4][WS_3(SEt)]$ (Boorman, P. M.; Wang, M.; Parvez, M. *J. Chem. Soc., Chem. Commun.* **1995**, 999−1000). We now report the isolation of a range of related compounds, with 1°, 2°, and 3° alkyl thiolate ligands, including one Mo example. $[PPh_4][WS_3(SR)]$ (R = ^{i}Bu (**1**), ^{i}Pr (**2**), ^{t}Bu (**3**), benzyl (**5**), allyl (**6**)) and $[PPh_4][MoS_3(S^tBu)]$ (**4**) have been isolated in fair to good yields from the reaction of $[PPh_4]_2[MS_4]$ with the appropriate alkyl halide in acetonitrile and subjected to analysis by X-ray crystallography. Crystal data are as follows: for **1**, triclinic space group $P\bar{1}$ (No. 2), a = 11.0377(6) Å, b = 11.1307(5) Å, c = 13.6286(7) Å, α = 82.941(1)°, β = 84.877(1)°, γ = 60.826(1)°, Z = 2; for **2**, monoclinic space group $P2_1/c$ (No. 14), a = 9.499(6) Å, b = 15.913(5) Å, c = 18.582(6) Å, β = 99.29(4)°, Z = 4; for **3**, monoclinic space group $P2_1/n$ (No. 14), a = 10.667(2) Å, b = 17.578(2) Å, c = 16.117(3) Å, β = 101.67(1)°, Z = 4; for **4**, monoclinic space group $P2_1/n$ (No. 14), a = 10.558(3) Å, b = 17.477(3) Å, c = 15.954(3) Å, β = 101.18(2)°, Z = 4; for **5**, monoclinic space group $P2_1/n$ (No. 14), a = 16.2111(9) Å, b = 11.0080(6) Å, c = 18.1339(10) Å, β = 111.722(1)°, Z = 4; for **6**, triclinic space group $P\bar{1}$ (No. 2), a = 9.4716(9) Å, b = 10.4336(10) Å, c = 14.4186(14) Å, α = 100.183(2)°, β = 90.457(2)°, γ = 91.747(2)°, Z = 2. Structures **3** and **4** are isomorphous, and **1** exhibits disorder about the tertiary carbon. **6** has been shown to exhibit fluxionality in solution by variable-temperature ^{1}H NMR studies, and an allyl migration mechanism is implicated in this process. The kinetics for the reaction of $[WS_4]^{2-}$ and EtBr were measured and suggest an associative nucleophilic substitution (S_N2) mechanism. The decomposition of the $[WS_3(SEt)]^-$ ion is shown to be second order with respect to this ion, suggesting the formation of a transient binuclear intermediate. M−S bond cleavage is the predominant step in decomposition of **1**−**6** to yield alkyl sulfides, alkyl thiols, and polythiometalates such as $[PPh_4]_2[M_3S_9]$. In contrast, reactions of $[PPh_4]_2[WO_xS_{4-x}]$ (x = 1, 2) with ^{t}BuBr result in the additional decomposition product of isobutene, presumably by C−S bond cleavage and β-hydrogen transfer. Interestingly, the reaction of $[PPh_4]_2[WOS_3]$ with BzCl yields **5** as the only isolable W thiolate species.

Introduction

Sulfur-ligated group 6 metal complexes have long been used in industrial settings as catalysts, photovoltaic materials, and lubricants and in batteries.[2] However, high oxidation state mononuclear thiolate complexes are still relatively rare, partly due to the tendency for reduction at the metal with formation of disulfides,[3] and also due to the ease with which sulfur ligands can bridge between metal centers. The result is the facile formation of polythiometalates from mononuclear thiometalates, where many structural architectures have previously been characterized.[3c,4]

From a biological point of view, sulfur-ligated molybdenum centers, and more recently tungsten centers, are known to exist at the active metal sites in a wide variety of enzymes.[5] Model complexes of tungsten and molybdenum have been used to simulate the coordination geometries of these centers with much success,[6] in many cases using large multidentate ligands to stabilize the metal center from reduction and polymetalate formation. For example, the tris pyrazolylborate ligand has been

(1) (a) Boorman, P. M.; Wang, M.; Parvez, M. *J. Chem. Soc., Chem. Commun.* **1995**, 999−1000. (b) Parvez, M.; Boorman, P. M.; Wang. M. *Acta Crystallogr.* **1997**, *C53*, 413−414.

(2) (a) Stiefel, E. I.; Matsumoto, K. *Transition Metal Sulfur Chemistry, Biological and Industrial Significance*; American Chemical Society: Washington, DC, 1996 and references therein. (b) Müller, A.; Krebs, B. *Sulfur: Its Significance for Chemistry, for the Geo-, Bio- and Cosmosphere and Technology*; Elsevier: Amsterdam, 1984 and references therein.

(3) (a) Gea, Y.; Greaney, M. A.; Coyle, C. L.; Stiefel, E. I. *J. Chem. Soc., Chem. Commun.* **1992**, 160−161. (b) Pan, W.-H.; Harmer, M. A.; Halbert, T. R.; Stiefel, E. I. *J. Am. Chem. Soc.* **1984**, *106*, 459−460. (c) Cohen, S. A.; Stiefel, E. I. *Inorg. Chem.* **1985**, *24*, 4657−4662.

(4) (a) Müller, A.; Bögge, H.; Krickemeyer, E.; Henkel, G.; Krebs, B. *Z. Naturforsch.* **1982**, *37b*, 1014−1019. (b) Chandrasekaran, J.; Ansari, M. A.; Sarkar, A. *Inorg. Chem.* **1988**, *27*, 3663−3665. (c) Sécheresse, F.; Lefebvre, J.; Daran, J. C.; Jeanin, Y. *Inorg. Chem.* **1982**, *21*, 1311−1314. (d) Greaney, M. A.; Stiefel, E. I. *J. Chem. Soc., Chem. Commun.* **1992**, 1679−1680.

(5) (a) Hille, R. *Chem. Rev.* **1996**, *96*, 2757−2816. (b) Johnson, M. K.; Rees, D. C.; Adams, M. W. W. *Chem. Rev.* **1996**, *96*, 2817−2839.

(6) Stiefel, E. I.; Coucouvanis, D.; Newton, W. E. *Molybdenum Enzymes, Cofactors and Model Systems*; American Chemical Society: Washington, DC, 1993 and references therein.

10.1021/ic000970n CCC: $20.00
Published on Web 05/19/2001

successfully used to isolate high valent tungsten complexes that show similarities in their metal coordination environment to enzymes such as formate dehydrogenase.[7] Recently, complexes with chelating dithiolenes and a bulky silyloxide ligand have been shown to simulate the metal environment in DMSO reductase,[8] in addition to exhibiting some oxygen atom transfer behavior. Much attention has also been given to the active site in the enzyme nitrogenase, which contains the bimetallic Fe/Mo/S cluster, FeMoco. A large number of FeMoco models have been synthesized,[2b,6] some of which can be derived from mononuclear thiometalates.[9] Many other simpler examples of thiometalates acting as metalloligands can be also be found in the literature.[10]

In vivo, Mo and W enzymes are known to acquire the respective metal in the form of metalate or thiometalate,[11,12] the former being converted to oxothiometalate before reaching the active center.[13] Such centers often include thiolate ligands (or selenolate in some cases),[5] and so it has been of interest to us to investigate the formation of C−S bonds using simple, unactivated mononuclear thiotungstates and thiomolybdates. We have found that although C−S bond formation on $[MS_4]^{2-}$ (M = Mo, W) can be achieved using alkyl halides, the alkylated species are generally unstable and behave as intermediates in the formation of polythiometalates and various organic sulfides. This has made for a complex system to investigate with respect to the sheer number of decomposition products formed. Yet despite this complexity, NMR solution studies have allowed us to identify the appropriate conditions to maximize the chances of isolating the pure thiolate intermediates. As a result we have been successful in isolating a number of tungsten examples and one molybdenum example of monoalkylated thiometalate(VI) complexes.

Experimental Section

General Procedures. All manipulations were performed under an atmosphere of dry dinitrogen or argon, using standard Schlenk and glovebox techniques. All solvents were distilled over appropriate drying agents[14] onto molecular sieves, and degassed with dinitrogen prior to use. All alkyl halides were purchased from Aldrich and stored over molecular sieves under dinitrogen. These were degassed by freeze−pump−thaw techniques prior to use. Thiometalates $[PPh_4]_2[MO_xS_{4-x}]$ (where M = Mo, W and $x = 0-2$) were prepared by a modified version of a literature procedure[15] and stored under dinitrogen. Elemental analyses were performed by the University of Calgary, Department of Chemistry, Analytical Services Laboratory. GC−MS data were recorded using a system consisting of a Packard Bell HP chromatograph equipped with a 5790 mass detector. ^{1}H and ^{13}C NMR spectra were recorded using Bruker ACT-200 or DRX-400 spectrometers. Time-dependent ^{1}H NMR studies were performed on either a Bruker AMX-300 or DRX-400 spectrometer. A typical experiment used 4 mg of $[PPh_4]_2[WS_4]$ dissolved in ca. 0.7 mL CD_3CN under dinitrogen in a 5 mm tube fitted with a rubber septum. An appropriate amount of alkylating agent was injected through the septum (while the sample was in an ice bath in some cases) and the sample returned to the probe to start data acquisition at predetermined intervals. ^{183}W measurements were performed using a wide-bore Bruker AM-400 spectrometer operating at a resonance frequency of 16.7 MHz and equipped with a horizontal solenoid probe. THF extract containing the appropriate alkylated species was used directly to prepare samples in cylindrical Pyrex tubes, with an outside diameter of 17 mm and a length of about 4 cm. The field stability of the Supercon made it possible to acquire all spectra unlocked. Spectra were referenced to an external standard of 2 M Na_2WO_4 in H_2O (δ (ppm) = (ν(sample) − $\nu(Na_2WO_4)$/$\nu(Na_2WO_4)$) × 10^6). All spectra were acquired at room temperature (21 ± 1 °C) with a pulse length of 20 μs (30° pulse), a relaxation time of 0.327 s, and a sweep width of 25 kHz. Generally, 16K complex data points were used for each pulse. Each sample was run twice to ensure reproducibility of the signal.

Synthetic Procedures. $[PPh_4][WS_3(S^iBu)]$ (1). $[PPh_4]_2[WS_4]$ (0.128 g, 0.129 mmol) was placed in a Schlenk tube and dissolved in ca. 20 mL of CH_3CN. A 10-fold excess of ^{i}BuBr (141 μL, 1.29 mmol) was added by syringe and the mixture stirred at room temperature. After 6 h, the yellow solution had turned orange, and the solvent and excess ^{i}BuBr were removed in vacuo. In addition, volatile byproducts of the formula $^iBu_2S_n$ (where $n = 1-3$) were removed by pumping. THF (2 × 20 mL) was used to extract the red residue to yield a red solution of **1**, leaving $[PPh_4]_2[W_3S_9]$ and unreacted $[PPh_4]_2[WS_4]$ behind. The THF solution was filtered, then concentrated to about half its original volume, placed in crystallization tubes, and layered with diethyl ether under dinitrogen. After 3 days, bright red crystals of crystallographic quality were obtained in a 63% yield. Anal. Calcd for $C_{28}H_{29}PS_4W$: C, 47.46; H, 4.12. Found: C, 47.47; H, 4.04. ^{1}H NMR (200 MHz, CD_2Cl_2): δ 7.99−7.57 (m, 20H, P*Ph*$_4^+$), 3.12 (d, 2H), 1.95 (m, 1H), 0.95 (d, 6H). ^{183}W NMR (400 MHz, THF): δ 3708 ppm.

$[PPh_4][WS_3(S^iPr)]$ (2). **2** was synthesized by a procedure similar to that used for **1** except that ^{i}PrBr was added (121 μL, 1.29 mmol) and the mixture stirred for 16 h before the solvent and volatiles were removed in vacuo. After the residue was extracted with THF (2 × 20 mL) and the solution concentrated to ca. 10 mL, diethyl ether (20 mL) was introduced to precipitate **2** as an orange red solid. After isolation, an 87% yield of **2** was obtained. Recrystallization from THF layered with diethyl ether resulted in red crystals of crystallographic quality. Anal. Calcd for $C_{27}H_{27}PS_4W$: C, 46.69; H, 3.92. Found: C, 47.06; H, 3.81. ^{1}H NMR (200 MHz, $CDCl_3$): δ 7.85−7.60 (m, 20H, P*Ph*$_4^+$), 3.70 (sept, 1H), 1.38 (d, 6H). ^{13}C{^{1}H} NMR (200 MHz, $CDCl_3$): δ 135.9, 134.9, 131.2, 116.8 (d, P*Ph*$_4^+$), 45.4 (*C*H), 26.0 (*C*H$_3$).

$[PPh_4][WS_3(S^tBu)]$ (3). **3** was synthesized by a procedure similar to that used for **1** except that ^{t}BuBr was added (28.2 μL, 0.258 mmol) and the mixture stirred for 8 h before the solvent and volatiles were removed in vacuo. The residue was extracted with THF (2 × 20 mL) to give a red solution, which was filtered, then layered with Et_2O, and maintained at −20 °C for a week. Red crystals of **3** were obtained in a 27% yield. Anal. Calcd for $C_{28}H_{29}PS_4W$: C, 47.46; H, 4.12. Found: C, 47.40; H, 4.06. ^{1}H NMR (200 MHz, $CDCl_3$): δ 7.85−7.60 (m, 20H, P*Ph*$_4^+$), 1.50 (s, 9H). ^{13}C{^{1}H} NMR (200 MHz, $CDCl_3$): δ 135.9, 134.9, 131.2, 116.8 (d, P*Ph*$_4^+$), 34.1 (*C*H$_3$).

$[PPh_4][MoS_3(S^tBu)]$ (4). $[PPh_4]_2[MoS_4]$ (0.400 g, 0.443 mmol) was placed in a Schlenk tube and dissolved in ca. 50 mL of CH_3CN. The solution was cooled to −30 °C, ^{t}BuBr (102 μL, 0.889 mmol) was added by syringe, and the mixture was allowed to warm to 0 °C. The mixture was stirred for 5 h, during which the color changed from bright red to black, with slight turbidity. The solvent and volatiles were removed in vacuo, and the solid was extracted with ice cold THF (2 × 20 mL). While maintained at 0 °C, the THF solution was filtered to remove fine black solid $[PPh_4]_2[Mo_3S_9]$ and then concentrated to half its original volume. After 3 days at −20 °C, black crystals of **4** were obtained in a 20% yield. Anal. Calcd for $C_{28}H_{29}MoPS_4$: C, 54.18; H, 4.71. Found: C, 53.63; H, 4.25. ^{1}H NMR (200 MHz, $CDCl_3$): δ 7.95−7.60 (m, 20H, P*Ph*$_4^+$), 1.49 (s, 9H). ^{13}C{^{1}H} NMR (200 MHz, $CDCl_3$): δ 135.9, 134.8, 131.1, 118.0 (d, P*Ph*$_4^+$), 34.1 (*C*H$_3$).

$[PPh_4][WS_3(SBz)]$ (5). **5** was synthesized by a procedure similar to that used for **1**, except that benzyl chloride (148 μL, 1.29 mmol), instead

(7) Eagle, A. A.; Tiekink, E. R. T.; Young, C. G. *Inorg. Chem.* **1997**, *36*, 6315−6322.
(8) Donahue, J. P.; Lorber, C.; Nordlander, E.; Holm, R. H. *J. Am. Chem. Soc.* **1998**, *120*, 3259−3260.
(9) Coucouvanis, D. *Acc. Chem. Res.* **1991**, *24*, 1−8.
(10) Müller, A.; Bögge, H.; Schimanski, U.; Penk, M.; Nieradzik, K.; Dartmann, M.; Krickemeyer, E.; Schimanski, J.; Römer, C.; Römer, M.; Dornfeld, H.; Wienböker, U.; Hellman, W.; Zimmermann, M. *Monatsh. Chem.* **1989**, *120*, 367−391.
(11) Fraùsto da Silva, J. J. R.; Williams, R. J. P. *The Biological Chemistry of the Elements*; Clarendon Press: Oxford, 1991; p 432.
(12) Müller, A.; Diemann, E.; Jostes, R.; Bögge, H. *Angew. Chem., Int. Ed. Engl.* **1981**, *20*, 934−955.
(13) Hall, D. R.; Gourley, D. G.; Leonard, G. A.; Duke, E. M. H.; Anderson, L. A.; Boxer, D. H.; Hunter, W. N. *EMBO J.* **1999**, *18*, 1435−1446.
(14) Perrin, D. D.; Amarego, W. L. F. *Purification of Laboratory Chemicals*, 3rd ed.; Pergamon Press: Oxford, 1988.
(15) Macdonald, J. W.; Friesen, G. D.; Rosenhein, L. D.; Newton, W. E. *Inorg. Chim. Acta* **1983**, *72*, 205−210.

Table 1. Crystallographic Data for [PPh4][WS3(SR)] (R = iBu (**1**), iPr (**2**), tBu (**3**), Bz (**5**), Allyl (**6**)) and [PPh4][MoS3(SR)] (R = tBu (**4**))

	1	2	3	4	5	6
empirical formula	$C_{28}H_{29}PS_4W$	$C_{27}H_{27}PS_4W$	$C_{28}H_{29}PS_4W$	$C_{28}H_{29}PS_4Mo$	$C_{31}H_{27}PS_4W$	$C_{27}H_{25}PS_4W$
mol wt (g mol^{-1})	708.57	694.57	708.57	620.69	742.59	692.53
color	red	red	red	dark brown	red	red
cryst syst	triclinic	monoclinic	monoclinic	monoclinic	monoclinic	triclinic
space group	$P\bar{1}$ (No. 2)	$P2_1/c$ (No. 14)	$P2_1/n$ (No. 14)	$P2_1/n$ (No. 14)	$P2_1/n$ (No. 14)	$P\bar{1}$ (No. 2)
a (Å)	11.0377(6)	9.499(6)	10.667(2)	10.558(3)	16.2111(9)	9.4716(9)
b (Å)	11.1307(5)	15.913(5)	17.578(2)	17.477(3)	11.0080(6)	10.4336(10)
c (Å)	13.6286(7)	18.582(6)	16.117(3)	15.954(3)	18.1339(10)	14.4186(14)
α (deg)	82.941(1)					100.183(2)
β (deg)	84.877(1)	99.29(4)	101.67(1)	101.18(2)	111.722(1)	90.457(2)
γ (deg)	60.826(1)					91.747(2)
V (Å^3)	1450.05(13)	2772(2)	2959.4(7)	2887(1)	3006.2(3)	1401.7(2)
Z	2	4	4	4	4	2
ρ_{calcd} (g cm^{-3})	1.623	1.664	1.590	1.472	1.641	1.641
T (K)	193	170	296	150	193	193
R[a]	0.0282	0.037	0.044	0.049	0.0409	0.0413
R_w[b]	0.0717	0.027	0.044	0.048	0.0659	0.0968
GOF[c]	1.015	1.38	1.72	2.96	0.819	0.976

[a] $R = \sum||F_o| - |F_c||/\sum|F_o|$. [b] For structures **1**, **5**, and **6**, $R_w = [\{\sum w(F_o^2 - F_c^2)^2\}/\sum w(F_o^4)]^{1/2}$; for structures **2**, **3**, and **4**, $R_w = [\{\sum w(|F_o| - |F_c|)^2\}/\sum wF_o^2]^{1/2}$. [c] For structures **1**, **5**, and **6**, $[\sum w(F_o^2 - F_c^2)^2/(n-p)]^{1/2}$ (n = number of data; p = number of parameters varied); for structures **2**, **3**, and **4**, $[\sum w(|F_o| - |F_c|)^2/(n-p)]^{1/2}$.

of iBuBr, was added at 0 °C and the mixture allowed to warm to room temperature. The solvent and volatiles were removed in vacuo after stirring for 2 h (Note: the mixture was only pumped until a sticky residue remained as pumping to complete dryness resulted in partial decomposition of **5**), and the residue was extracted with THF (2 × 20 mL) to give a red solution. After filtration, the solution was layered with Et_2O and maintained at −20 °C for 3 days. Bright red crystals of **5** were obtained in a 73% yield. Anal. Calcd for $C_{31}H_{27}PS_4W$: C, 50.14; H, 3.66. Found: C, 49.93; H, 3.55. ^{1}H NMR (200 MHz, CD_3CN): δ 7.97−7.60 (m, 20H, P*Ph*$_4^+$), 7.39−7.20 (m, 5H), 4.36 (s, 2H). ^{183}W NMR (400 MHz, THF): δ 3712 ppm.

[PPh4][WS3(SC3H5)] (6). 6 was synthesized by a procedure similar to that used for **1** except that allyl bromide (22 μL, 0.26 mmol), instead of iBuBr, was added at 0 °C and the mixture allowed to warm to room temperature. The solvent and volatiles were removed in vacuo after stirring for 2 h, and the residue was extracted with THF (2 × 20 mL) to give a red solution. After filtration, the solution was layered with Et_2O and maintained at −20 °C for 4 days. Bright red crystals of **6** were obtained in a 67% yield. Anal. Calcd for $C_{27}H_{25}PS_4W$: C, 46.83; H, 3.64. Found: C, 46.67; H, 3.57. ^{1}H NMR (400 MHz, CD_3CN, −40 °C): δ 7.95−7.62 (m, 20H, P*Ph*$_4^+$), 5.87 (m, 1H), 5.10 (d of m, 1H, cis to CH_2), 5.00 (d of m, 1H, trans to CH_2), 3.70 (d of m, 2H, C*H*$_2$).

Crystal Structure Determinations. Crystals of **1**, **5**, and **6** were coated in Paratone-8277 oil and then mounted on a glass fiber. Data were collected using a Bruker P4/RA diffractometer with a SMART 1000 CCD detector, using monochromated Mo Kα radiation at −80 °C. Programs for diffractometer operation, data collection, data reduction, and absorption correction were those supplied by Bruker. Data were integrated to a maximum 2θ value of 51.40° for **1** and **5**, and 51.60° for **6**. The data were corrected for absorption through use of Gaussian integration for **1** and **6**, and through use of the SADABS procedure for **5**. The structure of **5** was solved using the program SHELXS-86,[16] while the solutions for **1** and **6** were obtained though use of the DIRDIF-96 program system.[17] The structure refinements were completed by subsequent Fourier syntheses and refined using full-matrix least-squares methods.[18] All non-hydrogen atoms were refined anisotropically, and all hydrogen atoms were placed in idealized positions. In the structure of **1**, the isobutyl group exhibited disorder at the tertiary carbon. The alternate positions of this atom were refined satisfactorily with occupancy factors of 0.5.

Crystals of **2**, **3**, and **4** were mounted directly onto a glass fiber. Data were collected using a Rigaku AFC6S diffractometer with graphite-monochromated Mo Kα radiation at −103°, 23°, and −83 °C, respectively. Cell constants and an orientation matrix for data collection were obtained from a least-squares refinement using the setting angles of 25 centered reflections in the range ∼18° < 2θ < ∼25°. The data were collected using the $\omega-2\theta$ scan technique to a maximum 2θ value of 50.1°. An empirical absorption correction based on Gaussian integration was applied, and the data were also corrected for Lorentz and polarization effects. The structures were solved by direct methods,[17] completed by subsequent Fourier syntheses, and refined using full-matrix least-squares methods.[19] All non-hydrogen atoms were refined anisotropically, and all hydrogen atoms were placed in idealized positions.

Crystallographic parameters are given in Table 1, and additional data are available as Supporting Information.

Kinetics Experiments. Ethylation of [PPh4]2[WS4]. The reaction was studied via UV−vis spectra, which were obtained using a Varian 5E UV−vis−near-IR spectrophotometer equipped with a temperature-control unit to maintain a constant temperature (25 °C). Using a UV cell with a 1 cm path length and a maximum capacity of 6.0 mL, six runs were performed with various concentrations of reagents. The cell and the solutions were rigorously held under an atmosphere of dry nitrogen throughout the experiment. The following is a description of a typical run. $[PPh_4]_2[WS_4]$ (0.0960 g, 0.969 mmol) was dissolved in dry CH_3CN and diluted to 100 mL in a volumetric flask. The solution was further diluted 10-fold, giving a concentration of 9.69×10^{-5} M in $[WS_4]^{2-}$. For each run, an aliquot of 2−6 mL was syringed into the UV cell (fitted with a septum) and weighed before and after. An initial absorbance was recorded before ethyl bromide (EtBr) was added by syringe. After a quick mixing (a delay which was corrected for), the instrument started scanning at predetermined intervals. Spectra ranging from 350 to 550 nm were measured at equal intervals (10−15 min/cycle). These data (Figure 1) showed that two isosbestic points existed over the full time period of three half-lives for the reaction, indicating that the starting material, $[WS_4]^{2-}$, is stoichiometrically converted into the initial product, $[WS_3(SEt)]^-$. Hence we felt confident in carrying out a full kinetic analysis. Over longer periods, a red precipitate started to form in the cell, indicative of the conversion of the initial alkylated product into other species. The data from these scans were autosaved and processed using the commercial software package EASYPLOT. The main systematic errors were from weighing (5%) and measurement of small volumes of liquids.

(16) Sheldrick, G. M. *Acta Crystallogr.* **1990**, *A46*, 467−473.
(17) Beurskens, P. T.; Beurskens, G.; Bosman, W. P.; de Gelder, R.; Garcia Granda, S.; Gould, R. O.; Israel, R.; Smits, J. M. M. The *DIRDIF-96* program system; Crystallography Laboratory, University of Nijmegen: The Netherlands, 1996.
(18) Sheldrick, G. M. *SHELXL-93*. Program for crystal structure determination; University of Göttingen: Göttingen, Germany, 1993.
(19) *teXsan: Crystal Structure Analysis Package*; Molecular Structure Corporation: The Woodlands, TX, 1985 and 1992.

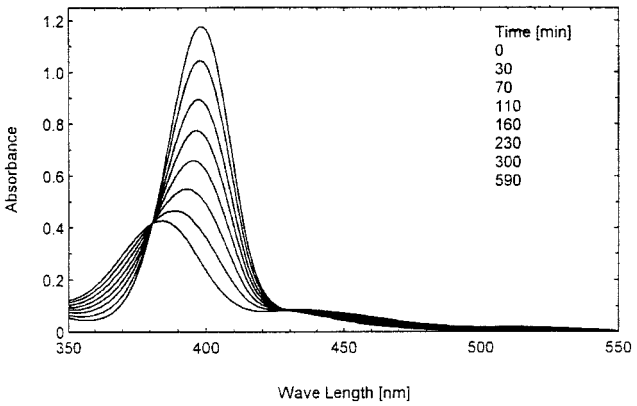

Figure 1. Electronic spectra of the reaction of EtBr + $[WS_4]^{2-}$ in CH_3CN at 25 °C; $[[WS_4]^{2-}] = 6.81 \times 10^{-5}$ M, $[EtBr] = 8.61 \times 10^{-3}$ M (trial 2).

A series of experiments were carried out at 25 °C in CH_3CN. The rate equation for the alkylation reaction is expressed as

$$-\mathrm{d}[[WS_4]^{2-}]/\mathrm{d}t = k[[WS_4]^{2-}]^m[EtBr]^n = k_{obs}[[WS_4]^{2-}]^m \quad (1)$$

$$k_{obs} = k[EtBr]^n, \quad \ln(k_{obs}) = n(\ln [EtBr]) + \ln k \quad (2)$$

The absorbance data for the $[WS_4]^{2-}$ ion, which were used to follow the reaction, were corrected for the absorbance of the product at that wavelength. The values of ϵ at 398 nm used are $\epsilon_1 = 1.74 \times 10^4$ cm^{-1} M^{-1} for $[WS_4]^{2-}$ and $\epsilon_2 = 5.77 \times 10^3$ cm^{-1} M^{-1} for $[PPh_4][WS_3(SEt)]$. The decay of the absorbance at 398 nm of $[WS_4]^{2-}$ reflects concentration decrease with time using varied concentrations of reagents, when EtBr was used in excess during the reaction. A plot of the 398 nm absorbance decay for trials 1−6 is available as Supporting Information.

For the determination of observed rate constants and the order with respect to $[WS_4]^{2-}$, a plot of ln $[[WS_4]^{2-}]$ vs time was prepared and shown to be linear, indicating that the alkylation reaction of $[WS_4]^{2-}$ with EtBr is first order for $[WS_4]^{2-}$. An observed rate constant ($k_{obs} = k[EtBr]$), when EtBr was in excess, was obtained for trial 2 from the slope of the plot of ln $[[WS_4]^{2-}]$ vs time. Six different concentrations of EtBr were used, and all k_{obs} values were obtained in a similar manner. The plot of ln $[[WS_4]^{2-}]$ vs time and the data from the six different trials are available as Supporting Information.

From the slope of a plot of $\ln(k_{obs})$ vs ln [EtBr], the value of n in eq 1 was determined. The slope is $0.89 \approx 1$, which indicates that the reaction is first order for EtBr as well. It was further derived that $k = 0.67$ M^{-1} min^{-1}. Overall, the total rate equation for alkylation of $[WS_4]^{2-}$ by EtBr is

$$\text{rate} = -\mathrm{d}[[WS_4]^{2-}]/\mathrm{d}t = 0.67[[WS_4]^{2-}][EtBr]\ M^{-1}\ min^{-1}$$

Thus the reaction is second order overall and typical of an S_N2 reaction.

Decomposition of $[PPh_4][WS_3(SEt)]$. ^1H NMR was used to monitor the decrease of the methylene proton resonance of $[WS_3(SEt)]^-$. The only potential interfering agent which might enhance decomposition of $[WS_3(SEt)]^-$ was H_2O, resulting in formation of ethyl thiol. Experiments used varying amounts of $[PPh_4][WS_3(SEt)]$ dissolved in ca. 0.7 mL of 1,1,2,2-tetrachloroethane-d_2 under dinitrogen in a 5 mm tube. 1,1,2,2-Tetrachloroethane-d_2 could be effectively dried prior to use with molecular sieves and consequently remove the risk of H_2O contamination, which is more of a problem in solvents such as CH_3CN. In addition, even in the presence of trace H_2O, formation of ethyl thiol has only been observed after extended periods of time, far in excess of the data collection period for this experiment. The probe was heated to 80 °C and the sample returned to the probe to start data acquisition at predetermined intervals. The concentration of $[WS_3(SEt)]^-$, which is proportional to the integration of the "CH_2" proton resonance, was normalized with respect to the integration value of the $[PPh_4]^+$ protons, which do not participate in the reaction. One mole of $[PPh_4][WS_3(SEt)]$ has an integration ratio of 20H in $[PPh_4]^+$ to 2H in CH_2. The mole ratio of CH_2 over $[PPh_4]^+$ becomes R_{Ph}, where $(PPh_4)_{intg}$ represents the value of proton integration of $[PPh_4]^+$ and $(CH_2)_{intg}$ represents the value of proton integration of "CH_2".

Scheme 1

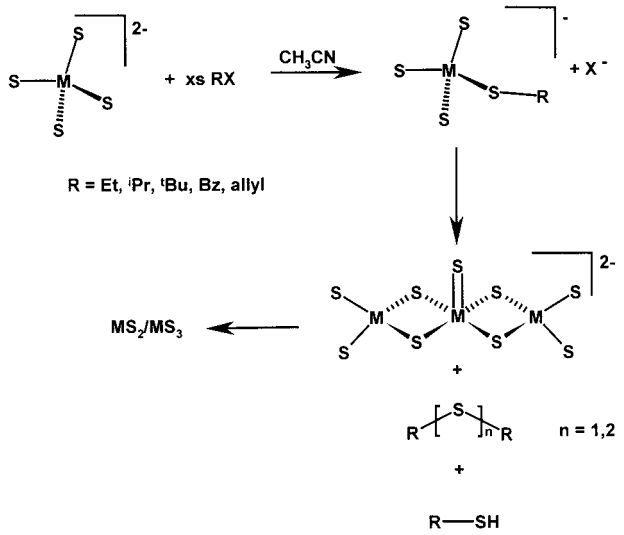

$$R_{Ph} = \frac{(CH_2)_{intg}}{2H}\frac{20H}{(PPh_4)_{intg}} = 10r \quad (3)$$

where

$$r = \frac{(CH_2)_{intg}}{(PPh_4)_{intg}}$$

The concentration of $[WS_3(SEt)]^-$, C, can be expressed as the ratio of integrations, where C_0 is equal to initial concentration of $[WS_3(SEt)]^-$.

$$C = C_0R_{Ph} = 10rC_0 \quad (4)$$

So, the decrease of $[WS_3(SEt)]^-$ with time can be fully described as the relationship of integration ratio (r) with time. A best-fit linear plot was obtained for $1/r$ vs time. Although there are only very small differences in the zero-, first-, and second-order best-fit lines, the residues of second order vs time give a more random distribution than the other possibilities. The experimental evidence thus justifies the conclusion that the decomposition of $[PPh_4][WS_3(SEt)]$ is a second-order reaction. Plots of r vs time and $1/r$ vs time, for trial 2, and numerical data for all three trials are available as Supporting Information.

The rate equation at 80 °C is considered as

$$\text{rate} = 0.05[[WS_3(SEt)]^-]^2\ M^{-1}\ min^{-1}$$

Results and Discussion

Our goal of isolating and characterizing the intermediate species from the irreversible alkylation of $[MS_4]^{2-}$ (M = Mo, W) was particularly challenging due to the varying instability of these species with respect to formation of organic sulfides, organic thiols, and condensed polythiometalates (Scheme 1). Formation of $[W_3S_9]^{2-}$ from $[WS_4]^{2-}$ in solution has previously been reported in the presence of ammonium, phosphonium, and arsonium salts, $[R_4X][Y]$ (where Y = OH, Cl, I),[20] and in the presence of alkyl halides (RX).[21] Although in each of these cases

(20) Von Hanewald, K.; Gattow, G. *Z. Anorg. Allg. Chem.* **1981**, *476*, 159−170.

(21) (a) Dhar, P.; Chandrasekaran, S. *J. Org. Chem.* **1989**, *54*, 2998−3000. (b) Dhar, P.; Ranjan, R.; Chandrasekaran, S. *J. Org. Chem.* **1990**, *55*, 3728−3729.

possible mechanisms have been suggested for the formation of the $[W_3S_9]^{2-}$ ion, no intermediates in these reactions had previously been isolated. In order to devise a synthetic strategy that would allow us to isolate these species, we required a better understanding of their formation and decomposition in situ. ^{1}H NMR spectroscopy provided an ideal handle for investigating these reactions in real time and consequently determining the optimum conditions for synthesis and isolation. By this approach, our initial studies involving alkylation reactions with ethyl halides were successful, and we were able to isolate the compound [PPh_4][WS_3(SEt)], including characterization by X-ray crystallography.[1] Successful isolation and characterization has since been achieved using primary, secondary, and tertiary halides for [PPh_4][WS_3(SR)] where R = ^{i}Bu, ^{i}Pr, ^{t}Bu, allyl, and Bz and for [PPh_4][MoS_3(SR)] where R = ^{t}Bu. Attempts to alkylate with adamantyl, vinyl, and phenyl halides were unsuccessful. With an interest to probing the mechanism of alkylation we have attempted to measure the kinetics for two of the reactions, using UV−vis spectroscopy.

Kinetics Experiments. The first reaction that we studied was that of $[WS_4]^{2-}$ and EtBr. We were able to monitor the disappearance of the yellow $[WS_4]^{2-}$ and formation of the red $[WS_3(SEt)]^-$, and obtain sufficient data points prior to significant decomposition of the alkylated species. This was shown quantitatively to be true from the presence of two well-defined and clean isosbestic points in the plot of the UV−vis spectra vs time (Figure 1). The reaction is first order in both $[WS_4]^{2-}$ and EtBr, indicating a classical, associative nucleophilic substitution mechanism (S_N2). We attempted to extend these kinetic studies to the ^{t}BuBr case, but were hampered by significant loss of alkylated product by decomposition. However, using only early data points, we were able to obtain data that suggested that the reaction is first order in ^{t}BuBr and zero order in $[WS_4]^{2-}$. This would be consistent with the dissociative nucleophilic mechanism (S_N1) expected for a tertiary alkyl halide, which normally forms a carbocation prior to nucleophilic attack, in contrast to a primary alkyl halide. For reactions of ^{i}BuBr, the isolated alkylated product contains only the ^{i}Bu alkyl group and formation of ^{t}Bu product is notably absent during the reaction. This is in agreement with the observation that a primary alkyl halide reacts by an S_N2 mechanism, since S_N1 would result in isomerization to the more stable ^{t}Bu before alkylation. Our lack of observed reaction for vinyl and phenyl halides is not surprising since neither will undergo nucleophilic substitution. As for adamantyl halides, it seems likely that the required planar transition state at the α-carbon cannot be achieved, so preventing a dissociative mechanism from occurring.

Synthesis. Isolation and Reactivity. Due to the sensitive nature of the alkylated species in solution to oxidative decomposition, reactions were all performed under an inert atmosphere. Decomposition due to aerial oxygen yields the usual organic sulfides and polythiometalates, in addition to [PPh_4]$_2$[W_6O_{19}] over long periods of time.[22] In some cases, the presence of moisture results in organic thiols being the predominant decomposition products. ^{1}H NMR has been successfully used to determine the optimum temperature and reaction time for alkylation reactions, to offer the best chance of isolation of these species. Figure 2 illustrates a typical alkylation reaction of [PPh_4]$_2$[WS_4] followed by NMR, in this case using benzyl chloride injected at 0 °C and then maintained at room temperature for the remainder of the experiment. The chemical shifts of the methylene protons in the various chemical environments

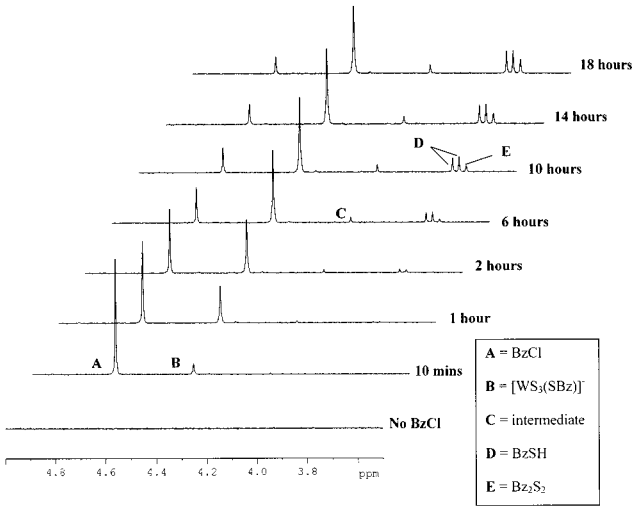

Figure 2. Time-dependent ^{1}H NMR series for [PPh_4]$_2$[WS_4] + BzCl in CD_3CN at room temperature.

are sufficiently well-defined to allow identification of various species in solution. The series of spectra clearly shows the benzyl chloride (BzCl, 4.67 ppm) being consumed (1 equiv) and the formation of the alkylated species at a more upfield position (4.36 ppm). The major organic decomposition product in this case is benzyl thiol (BzSH, 3.74 ppm, doublet, $^3J_{HH}$ = 7.7 Hz), which originates from the reaction of the alkylated species with the small amount of residual water present in the deuterated solvent. The signal at 3.70 ppm represents benzyl disulfide (Bz_2S_2), and the additional decomposition peak at 4.05 ppm is believed to be due to an as yet unidentified intermediate, which we have independently generated by the reaction of Bz_2S_2 and $[WS_4]^{2-}$, or Bz_2S_2 and $WS_3(SBz)^-$. From these data, we can deduce that the optimum reaction time, when *1 equiv* of benzyl chloride is used at room temperature, is 10 h. When a large excess of benzyl chloride is used, the optimum reaction time is reduced to 2 h, and significant decomposition has not occurred by this time, making a more desirable set of reaction conditions.

Time-dependent ^{1}H NMR studies of the first stage in the decomposition of $[WS_3(SEt)]^-$ suggested that the process required the association of two such ions to give Et_2S_2 as the major initial organosulfur product. Such a mechanism would therefore show second-order kinetics in terms of $[WS_3(SEt)]^-$, with the reciprocal of concentration of $[WS_3(SEt)]^-$ having a linear relationship with time. In addition, the observation that the decomposition process is greatly accelerated by increasing the concentration of $[WS_3(SEt)]^-$ in solution is in agreement with the suggestion of second-order kinetics. Our UV−vis spectral study of the ethylation of $[WS_4]^{2-}$, described above, indicated that formation of precipitates toward the end of the reaction might interfere with the accuracy of a decomposition study of this technique. We therefore decided to study the decomposition kinetics using ^{1}H NMR, by following the distinctive methylene proton resonances of the ethyl group in various chemical environments. Our kinetic measurements show that the rate is second order in $[WS_3(SEt)]^-$, which is suggestive that the first step in decomposition is the association of two ions and the subsequent reductive elimination of Et_2S_2. Attempts to isolate the resultant transient dinuclear species have been unsucessful. At room temperature, prolonged standing of this $[WS_3(SEt)]^-$ solution leads to a dark oily red material or to black or dark brown precipitates, especially when the concentration is above 0.01 M. One sample of these dark precipitates

(22) Parvez, M.; Boorman, P. M.; Langdon, N. L. *Acta Crystallogr.* **1998**, *C54*, 608−609.

Table 2. Selected Bond Lengths (Å) and Bond Angles (deg) for $[PPh_4][WS_3(SR)]$ (R = ^{i}Bu (**1**), ^{i}Pr (**2**), ^{t}Bu (**3**), Bz (**5**), Allyl (**6**)) and $[PPh_4][MoS_3(SR)]$ (R = ^{t}Bu (**4**))

	1	**2**	**3**	**4**	**5**	**6**
M−S(1)	2.3231(10)	2.326(3)	2.354(4)	2.341(2)	2.3376(18)	2.3295(18)
M−S(2)	2.1499(11)	2.153(3)	2.1514(3)	2.148(2)	2.1475(18)	2.1583(16)
M−S(3)	2.1476(13)	2.159(2)	2.144(4)	2.147(2)	2.1523(17)	2.1530(17)
M−S(4)	2.1471(13)	2.154(3)	2.143(4)	2.148(2)	2.1532(19)	2.1538(18)
S(1)−C(1)	1.825(5)	1.833(9)	1.86(2)	1.882(8)	1.819(7)	1.850(7)
S(1)−M−S(2)	109.87(5)	108.1(1)	110.0(2)	109.96(8)	109.58(7)	109.59(7)
S(1)−M−S(3)	102.80(5)	111.43(9)	99.8(2)	101.16(8)	102.89(7)	104.43(7)
S(1)−M−S(4)	109.33(5)	104.6(1)	110.8(2)	111.40(9)	109.88(8)	109.39(7)
S(2)−M−S(3)	111.06(5)	109.5(1)	111.5(2)	111.79(8)	110.74(7)	110.57(7)
S(2)−M−S(4)	110.03(5)	111.9(1)	111.4(2)	110.09(8)	110.63(7)	110.65(8)
S(3)−M−S(4)	113.50(7)	111.3(1)	112.7(2)	112.17(9)	112.84(7)	112.02(8)
M−S(1)−C(1)	104.85(18)	108.7(3)	111.8(5)	111.8(2)	106.3(3)	103.9(2)

was identified as a mixture of WS_2/WS_3. As in the case of the alkylation kinetics discussed above, there is indirect evidence that the decomposition of $[WS_3(S^tBu)]^-$ is different from the decomposition of the primary alkyl analogues, notably through the distribution of organosulfur products. The system was intractable to study kinetically, however, due to the extremely rapid decomposition of the first intermediate.

We have found that the THF extract containing the alkylated species will partially decompose when left as a concentrated solution for prolonged periods of time at room temperature or if pumped to dryness in vacuo. As a result, we have successfully isolated these species using diethyl ether, either by precipitation or by layering of the concentrated THF solution, to give a crystalline material. In general, a rapid workup procedure for these products is the key to their successful isolation. In the analogous Mo chemistry, the alkylated species were found to be unstable at room temperature and so a low-temperature workup was necessary. The rapid decomposition of the Mo alkylated species, compared to the W species, may be explained by the greater tendency for the metal to be reduced, in addition to the weaker Mo−S bond.[24] This may also explain the observed formation of MoS_2 at room temperature, whereas WS_2 only forms when the reaction mixture is heated (except in the case of BzBr) for the respective W reactions.

Reactions investigating the alkylation of $[PPh_4]_2[MSe_4]$ (M = Mo, W)[24] have shown that similarities exist between the Mo/S and W/Se systems in both the rapidity with which the reaction proceeds and the instability of the alkylated products at room temperature, resulting in formation of MoS_2 and WSe_2, respectively. Such similarities appear to be due to similar redox behavior, as previously observed by Stiefel et al. with respect to induced internal electron transfer reactions using alkyl disulfides.[3a] During alkylation reactions of $[PPh_4]_2[MoS_4]$, the alkyl disulfides formed by degradation of the alkylated product subsequently react with residual $[MoS_4]^{2-}$. Such reactivity has also been observed with reactions of $[PPh_4]_2[WS_4]$, except on a much longer time scale.

Chlorinated solvents such as CH_2Cl_2 and $CHCl_3$ have been avoided due to their decomposing effect on both the thiometalates and alkylated products over time. It is likely that these solvents are actually behaving as alkylating agents, forming highly unstable methylated intermediates that rapidly decompose. At this point, we have been unable to isolate methylated intermediates from $[PPh_4]_2[WS_4]$ and CH_3Br due to their instability. Alkyl chlorides have been observed to react more slowly than their respective bromides, as expected for a nucleophilic substitution mechanism. As a result we have routinely used alkyl bromides to increase reaction rates and reduce the amount of time during which the alkylated species is in solution prior to workup, thereby reducing the period during which decomposition can occur. One exception is benzyl bromide, which reacts so rapidly that, as soon as the reaction mixture is concentrated in preparation for THF extraction, the red solution rapidly precipitates a dark solid, identified as WS_2. We have consequently used benzyl chloride in this case, which still reacts rapidly enough to isolate the alkylated species before significant decomposition can occur. Attempts to use alkyl iodides have been less successful, resulting in rapid decomposition of any transient alkylated product. This is believed to be partly due to the enhanced reaction rate of the iodide substitution, but also due to its redox behavior. We have previously isolated $[PPh_4][I_3]$ as a byproduct from the reaction of $[PPh_4]_2[WS_4]$ with CH_3I,[25] and such an oxidation would likely enhance reduction of alkylated products to the mixed oxidation state metalate $[PPh_4]_2[W_3S_9]$.

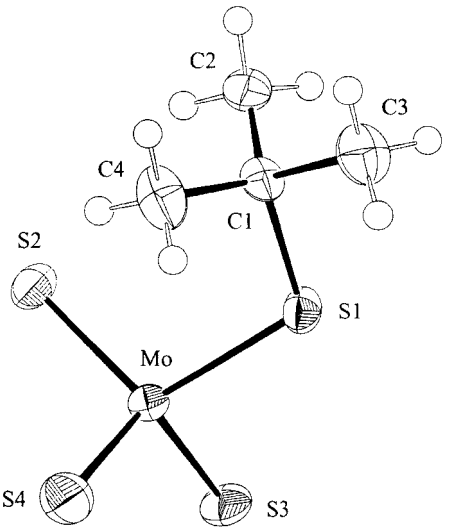

Figure 3. ORTEP representation and labeling scheme for the anionic portion of $[PPh_4][MoS_3(S^tBu)]$ (**4**), which is isostructural with the W analogue.

X-ray Crystallography. Selected bond distances and angles for **1**−**6** are shown in Table 2, and selected ORTEP representations are shown in Figures 3 and 4. The structures consist of $[PPh_4]^+$ cations and $[MS_3(SR)]^-$ (M = Mo, W; R = ^{i}Bu, ^{i}Pr, ^{t}Bu, Bz, C_3H_5) anions. The absence of any solvate molecules is in contrast to the R = Et structure,[1] which contains a molecule

(23) Gonzalez-Blanco, O.; Branchadell, V.; Monteyne, K.; Ziegler, T. *Inorg. Chem.* **1998**, *37*, 1744−1748.
(24) Kruhlak, N. L.; Boorman, P. M. Unpublished results.
(25) Parvez, M.; Wang, M.; Boorman, P. M. *Acta Crystallogr.* **1996**, *C52*, 377−378.

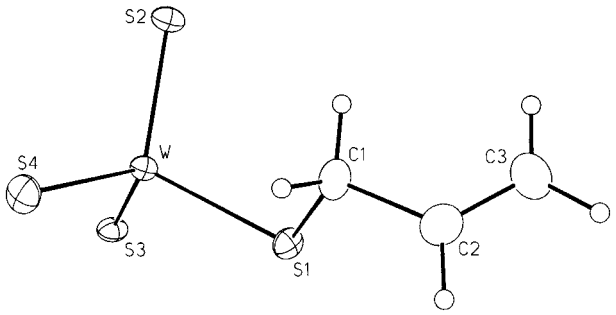

Figure 4. ORTEP representation and labeling scheme for the anionic portion of $[PPh_4][WS_3(SC_3H_5)]$ (**6**).

Table 3. Average and Representative Bond Distances (Å) for **1**−**6** and Related Compounds

compound	$M-S_{terminal}$	$M-S_{thiolate}$	S−C	ref
$[PPh_4][WS_3(SEt)]$	2.153 (av)	2.323(3)	1.86(1)	1a
$[PPh_4][WS_3(S^iBu)]$ (**1**)	2.148 (av)	2.3231(10)	1.825(5)	*a*
$[PPh_4][WS_3(S^iPr)]$ (**2**)	2.155 (av)	2.326(3)	1.833(9)	*a*
$[PPh_4][WS_3(S^tBu)]$ (**3**)	2.146 (av)	2.354(4)	1.86(2)	*a*
$[PPh_4][MoS_3(S^tBu)]$ (**4**)	2.148 (av)	2.341(2)	1.882(8)	*a*
$[PPh_4][WS_3(SBz)]$ (**5**)	2.151 (av)	2.3376(18)	1.819(7)	*a*
$[PPh_4][WS_3(SC_3H_5)]$ (**6**)	2.155 (av)	2.3295(18)	1.850(7)	*a*
$[PPh_4][WS_3(SH)]^b$	2.171(2)	2.171(2)		1b
$[PPh_4]_2[WS_4]$	2.195 (av)			27
$[PPh_4]_2[MoS_4]$	2.180 (av)			27
$Cp^*WS_2(S^tBu)$	2.147(2)	2.345(2)	1.850(9)	26a
$Cp^*WS_2(SBz)$	2.149 (av)	2.328(4)	1.861(1)	26a
$Cp^*MoS_2(S^tBu)$	2.136(1)	2.354(1)	1.874(5)	26b
$Cp^*Mo(S^tBu)_3$		2.296 (av)	1.871 (av)	26b
$[PPh_4][Cp^*WS_3]$	2.192 (av)			26b
$[PPh_4][Cp^*MoS_3]$	2.188 (av)			26b
$W(S^tBu)_4$		2.236(4)	1.871(18)	28a
$Mo(S^tBu)_4$		2.235(3)	1.84(2)	28b

[a] This work. [b] Thiol proton is disordered over four crystallographically equivalent sites.

of THF in the unit cell. The two ^{t}Bu structures, **3** and **4**, are isomorphous. The ^{i}Bu structure (**1**) exhibits disorder of the tertiary carbon (C2) and has been modeled satisfactorily using occupancy factors of 0.5 for each of the two sites. In all cases, the geometry at the metal center is approximately tetrahedral and the bond lengths and angles fall in the ranges for related structures (see Table 3). The $[PPh_4]^+$ cations are unremarkable and show no close contacts with the anions.

The average $M-S_{terminal}$ bond distances for $[PPh_4][MS_3(SR)]$ (M = Mo, W; R = Et, ^{i}Bu, ^{i}Pr, ^{t}Bu, Bz, C_3H_5) range from 2.146 to 2.155 Å and compare favorably with those of the analogous $Cp^*MS_2(SR)$ (M = Mo, W; R = ^{t}Bu, Bz),[26] which range from 2.136 to 2.149 Å (Table 3). It is noted that $[MS_3(SR)]^-$ exhibits terminal Mo−S and W−S distances that are almost identical, in contrast to the Cp* analogues which exhibit shorter terminal Mo−S distances than W−S, as also observed in the compounds $[PPh_4]_2[MS_4]$[27]and $[PPh_4][Cp^*MS_3]$ (M = Mo, W).[26b] In the case of $[MS_3(SH)]^-$, a M−S bond distance of 2.171(2) Å is observed;[1b] however, this apparent lengthening is due to disorder of the thiol proton over the four S sites, giving an average distance of three $M-S_{terminal}$ and one S−H.

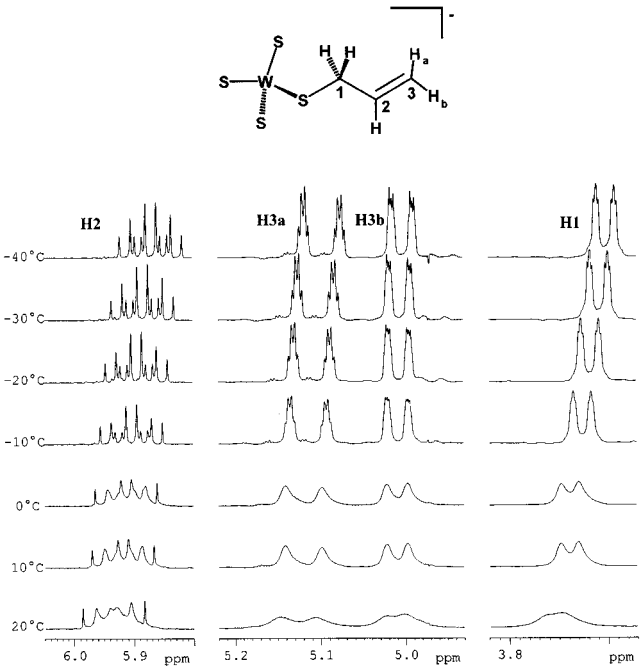

Figure 5. Variable-temperature ^{1}H NMR series for **6** in CD_3CN.

It is apparent that as the number of terminal sulfides increases on a single metal center, the amount of π-donation that each can provide is reduced, thus lengthening the $M-S_{terminal}$ bond distances. In reverse, structural data for Cp* polythiolate compounds shows that as the number of thiolate ligands increases, the $M-S_{thiolate}$ bond distance becomes shorter. It appears that the lack of competing π-donation from terminal sulfides allows more donation from the thiolate, thus shortening the $M-S_{thiolate}$ bonds. In the M(IV) compounds $M(S^tBu)_4$ (M = Mo, W), the π-donation is less pronounced due to the partially filled d orbitals on the metal.

The slight variations in $M-S_{thiolate}$ bond distances in $[MS_3(SR)]^-$ (M = Mo, W; R = Et, ^{i}Bu, ^{i}Pr, ^{t}Bu, Bz, C_3H_5) are likely due to the nature of the alkyl group present. The effect appears to be predominantly steric, with the bulky ^{t}Bu structures exhibiting the longest $M-S_{thiolate}$ bonds and no apparent lengthening due to the presence of electron-withdrawing Bz or allyl groups. The steric bulk of the alkyl groups is also reflected in the M−S−C bond angles, where the largest value is observed for ^{t}Bu (111.8(5)° and 111.8(2)° for W and Mo, respectively) and the smallest for allyl (103.9(2)°).

The S−C bond distances compare favorably with other related structures containing one or more thiolate ligands. The S−M−S angles vary by ca. 11° in each structure, with the smaller angles at S(1) reflecting the presence of the thiolate ligand.

Allyl Fluxionality. Temperature-dependent ^{1}H NMR studies of $[PPh_4][WS_3(SC_3H_5)]$ reveal that a fluxional process is occurring at room temperature (Figure 5). The signals become more resolved at −40 °C, with H2 becoming the clearest. While rotation about the C−S and/or C−C single bonds could result in broadened signals, such a phenomenon is not observed for any of the other alkyl groups investigated, and it would seem unlikely that H2 would become best resolved at low temperature if this process were occurring. Fluxionality where α and γ carbons are exchanged would result in enhanced resolution for H2 over H1 and H3 consistent with our observations. This could occur by two possible mechanisms (Figure 6): (a) α and γ carbons exchange via a four-membered cyclic transition state involving the same sulfur atom at all times, or (b) the allyl group migrates over the four sulfurs via a six-membered cyclic

(26) (a) Kawaguchi, H.; Tatsumi, K. *J. Am. Chem. Soc.* **1995**, *117*, 3885−3886. (b) Kawaguchi, H.; Yamada, K.; Lang, J.-P.; Tatsumi, K. *J. Am. Chem. Soc.* **1997**, *119*, 10346−10358.
(27) Kruhlak, N. L.; Nguyen, P. N.; Boorman, P. M.; Parvez, M. Manuscript in preparation.
(28) (a) Listemann, M. L.; Dewan, J. C.; Schrock, R. R. *J. Am. Chem. Soc.* **1985**, *107*, 7207−7208. (b) Otsuka, S.; Kamata, M.; Hitotsu, K.; Higuchi, T. *J. Am. Chem. Soc.* **1981**, *103*, 3011−3014.

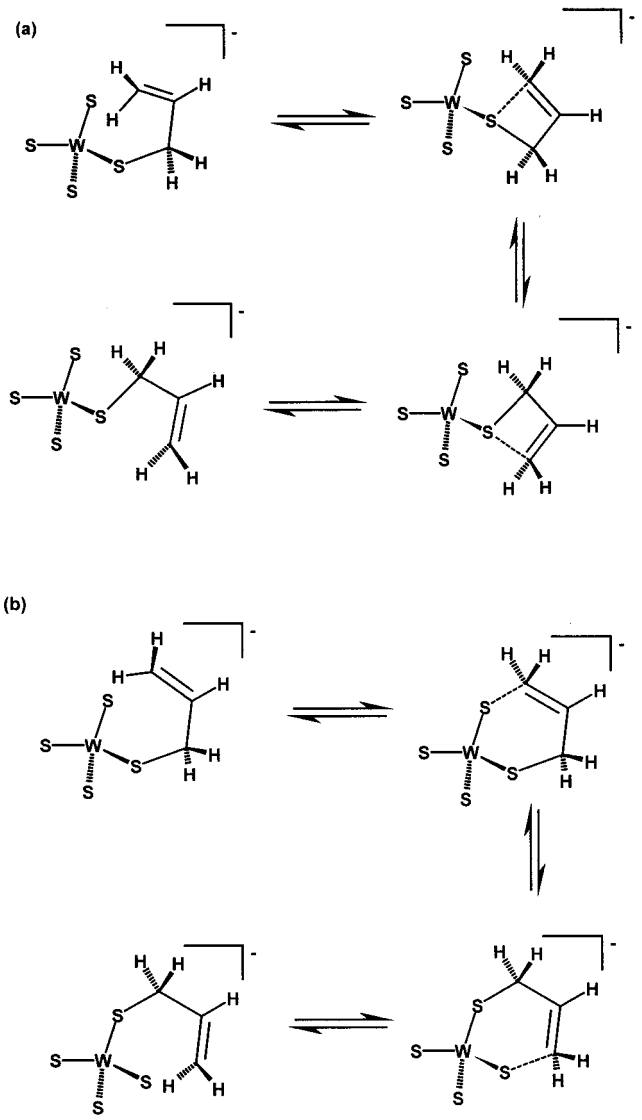

Figure 6. Possible modes of fluxionality in **6**.

transition state. Our current data does not allow us to determine which of these two mechanisms is occurring; however, the allyl migration over all four sulfurs is more attractive due to the more sterically accessible transition state invoked.

Reactions of Oxothiometalates. In view of the fact that the mixed oxothiometalates may well be important species in the biological uptake of Mo and W, it was of interest to examine their reactions with alkyl halides. Of the two possible alkylation sites it was expected that a preference would be shown for S rather than O. NMR studies of the reaction of BzCl with $[PPh_4]_2[WO_2S_2]$ and $[PPh_4]_2[WOS_3]$ implied this to be the case, on the basis of the similarity of the chemical shifts of the methylene protons to those observed in the tetrathiotungstate system. However, we have been unable to isolate any mixed oxothio(alkylthio)tungstate products. Instead when pure $[PPh_4]_2[WOS_3]$ was reacted with BzCl, the isolable alkylated product was $[PPh_4][WS_3(SBz)]$. We are confident that the observed product is not a consequence of the $[PPh_4]_2[WOS_3]$ being contaminated with $[PPh_4]_2[WS_4]$, since all reactions were performed with crystalline samples of $[PPh_4]_2[WOS_3]$. Analysis of the $[PPh_4]_2[WOS_3]$ crystals by X-ray crystallography confirmed that cocrystallization with $[PPh_4]_2[WS_4]$ was not occurring,[27] and since $[PPh_4]_2[WS_4]$ crystallizes in a different space group, as a microcrystalline solid under these conditions, we believe that our $[PPh_4]_2[WOS_3]$ sample was uncontaminated. It appears that the alkylation step initiates the redistribution of oxo and thio ligands, a phenomenon that is not observed in this system in the absence of alkyl halide.

A second surprising feature of the oxothiometalate reactions with alkyl halides was observed in reactions with ^{t}BuBr. It is quite clear that although C−S bond formation readily occurs when $[MS_4]^{2-}$ reacts with RX, the decomposition pathway proceeds by M−S bond cleavage. In the case of alkylation of $[PPh_4]_2[WO_2S_2]$ and $[PPh_4]_2[WOS_3]$ with ^{t}BuBr, we observed the formation of a small amount of isobutene, as detected both by GC−MS of the headspace gas in the reaction vessel and by time-dependent ^{1}H NMR studies. This suggests that C−S bond formation, and subsequent cleavage, is occurring only when an oxo ligand is present, by elimination of an unsaturated organic fragment and concomitant β-hydrogen transfer to a terminal oxo or thio ligand on the same metal center. The only precedent we have observed for this behavior is that $[PPh_4][WS_3(SH)]$ has previously been isolated from the reaction of $[PPh_4][WS_3(SEt)]$ and CuCl,[1b] which presumably resulted in elimination of ethylene. The analogous reaction involving $[PPh_4][WS_3(^tBu)]$ yielded isobutene as a byproduct. In these cases, however, the initial coordination to copper is necessary to stimulate alkene elimination.

Conclusions

We have demonstrated that alkylation of $[MS_4]^{2-}$ (M = Mo, W) using alkyl halides results in the formation of the transient $[MS_3(SR)]^-$ (R = ^{i}Bu, ^{i}Pr, ^{t}Bu, benzyl, allyl), which can be isolated as a $[PPh_4]^+$ salt under controlled conditions. These conditions have been identified by time-dependent ^{1}H NMR studies, which have also provided insight into the stability and decomposition pathways to polythiometalates, organic sulfides, and thiols. Alkylation by EtBr can be measured by UV−vis spectroscopy and has been shown to occur by an associative nucleophilic substitution (S_N2) mechanism. This appears to be in contrast to alkylation by bulkier alkyl groups such as ^{t}Bu, as expected for this type of reaction, and explains the inactivity of phenyl and vinyl halides toward $[MS_4]^{2-}$. Decomposition kinetics can be measured using ^{1}H NMR and, in the case of $[MS_3(SEt)]^-$, suggest that a second-order process in the anion is occurring, which is consistent with formation of a binuclear thiometalate and subsequent elimination of ethyl disulfide. The decomposition pathway appears to be dependent on the nature of the alkyl group since different ratios of organic sulfides and thiols are observed for different alkylating agents.

Attempts to alkylate $[WO_xS_{4-x}]^{2-}$ have not resulted in isolation of $[PPh_4][WO_xS_{3-x}(SR)]$; instead it appears that O/S ligand substitution is initiated by this process: we have isolated $[PPh_4][WS_3(SBz)]$ from the reaction of $[PPh_4][WOS_3]$ and BzCl. Furthermore, in contrast to $[MS_4]^{2-}$, reactions of ^{t}BuBr result in some C−S instead of M−S bond cleavage occurring and the elimination of an unsaturated organic fragment. Clearly, oxothiometalates react by a more complex route than the better understood tetrathiometalates.

Acknowledgment. We thank Dr. Deane McIntyre and Dr. Hans Vogel in the Department of Biological Sciences, University of Calgary, for the acquisition of ^{183}W NMR spectra. We also thank the University of Calgary and NSERC for financial support.

Supporting Information Available: Kinetic data described in the text, ORTEP representations for complexes **3**, **4**, and **6**, and X-ray crystallographic files in CIF format for complexes **1**−**6**. This material is available free of charge via the Internet at http://pubs.acs.org.

IC000970N